Tangential SX Imaging for Visualization of Fluctuations in Toroidal Plasmas

Satoshi OHDACHI, Kazuo TOI, Gerhard FUCHS[1)] and the LHD experimental Group

National Institute for Fusion Science, 509-5292, Japan

[1)]*Institut fuer Plasmaphysik, Forschungszentrum Juelich, D-52425, Germany*

(Received 20 December 2006 / Accepted 16 May 2007)

When the ratio of the plasma pressure to the magnetic pressure increases, Various kinds of instabilities evolve. Among them, magnetohydrodynamic instabilities, by which the plasma is deformed macroscopically, are in concern. Non-linear evolution of them is fairly complicated and two-dimensional structure of them is the key to understanding the phenomena. Tangentially viewing SX camera is promising diagnostics for 2D visualization, because most of the perturbations tend to have the equal phase along the field lines, the tangential view, which is almost parallel to the field lines, give a good opportunity to resolve the structure. Issues in this kind of camera are discussed. Improved system using multi-layer mirror is also described.

Keywords: imaging diagnostics, soft X-ray radiation, MHD instabilities, multi-layer mirror

DOI: 10.1585/pfr.2.S1016

1. Introduction

In magnetically confined fusion devices, the plasma is confined by the nested magnetic surfaces. In order to realize economical fusion reactors, reduction of the strength of the magnetic field is required. However, when the plasma β, the ratio of the plasma pressure to the magnetic pressure increases, various kinds of instabilities evolve. Among them, magnetohydrodynamics (MHD) instabilities, by which the plasma is deformed macroscopically, are in concern. MHD instabilities are well understood within the scope of the linear MHD theory; the threshold values of the plasma parameters for the appearance of the instabilities agree well with the predicted ones. However, evolution of them and its relation to the transport phenomena is fairy complicated and was not satisfactorily understand so far. Experimental study is therefore required. Measurements of the two dimensional (2D) structure of them might be the key elements in understanding the evolution of the instabilities. Sawtooth activities are a good example where the 2D measurement is essential. Recent results from the 2D ECE-imaging clearly show that toroidally localized magnetic reconnection causes the rapid transport observed in the sawtooth crash events [1]. Theoretical model, therefore, will be restricted more than any other measurements could do. In this sense, imaging diagnostics can be the most important diagnostics for the study of the macroscopic MHD instabilities.

Measurement of the Soft X-ray (SX) radiation profile is another candidate for studying 2D structure of the instabilities. Intensity of the SX radiation is rather complicated function of the electron density, the electron temperature and the impurity density. However, since the plasma parameters are constant on a magnetic surface, the iso-radiation surface can be a good estimate of the magnetic surface; deformation of the magnetic surfaces from the MHD instabilities can be studied from the shape of the iso-radiation surface. 2D Radiation profiles have been studies mainly by the tomographic reconstruction where many detectors surrounding the plasma are used [2–6]. We have developed another type of diagnostics, tangentially viewing SX cameras system, to study the 2D structure from the SX radiation [7]. Only one camera is needed in this method; installation of the camera system is much simpler. Though measured tangential images are line-integrated ones, images at a poloidal cross section can be directly estimated because most of the perturbations tend to have the equal phase along the field lines. In other words, the tangential view, which is almost parallel to the field lines, gives a good opportunity to resolve the structure [8]. This kind of camera system has been developed since early 80 s [9–11]. However, it became possible to measure the fluctuations of the plasma after we adopt the large diameter scintillator and the fast framing visible camera, which was available late 90 s. It is noted that similar type of SX camera system developed by different groups also began to work simultaneously [12, 13].

In this paper, we will show that how tangentially viewing camera system can detect the 2D structure appears in the magnetically confined plasmas. We then discuss the magnetic configurations where this kind of diagnostics can work well. Future improvements of camera system to study the fluctuations with higher mode number will be proposed finally.

author's e-mail: ohdachi@nifs.ac.jp

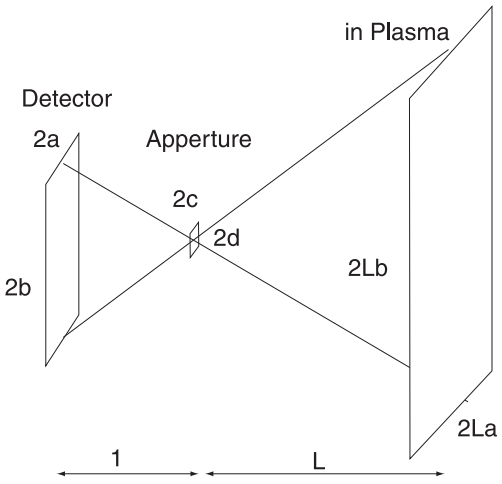

Fig. 1 Layout of the pinhole camera system.

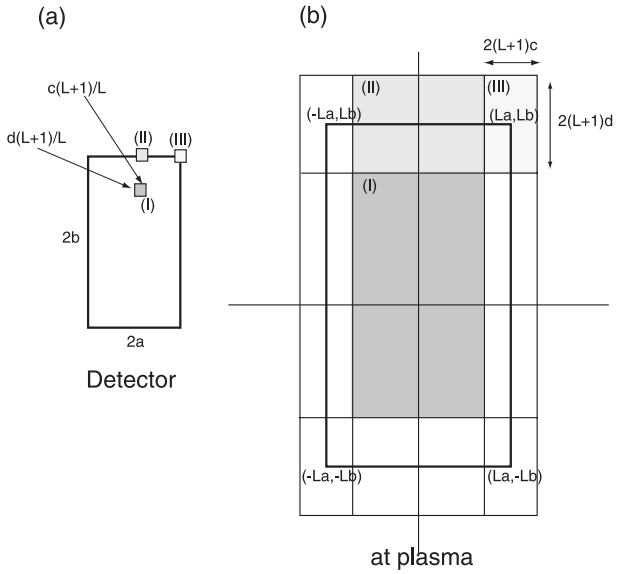

Fig. 2 Three cases where light from the plasma enters the detector.

2. Simulated Images with Diffrent Magnetic Configulations

Tangentially viewing SX camera, we have developed, basically is a pinhole camera having a fast framing video camera equipped with a scintillator screen for the soft X-ray detection. It can record tangential image with a framing rate up to 20 kHz [7]. Let us consider the effective brightness of a pinhole camera system with a configuration shown in the Fig. 1, where a rectangular detector and a rectangular aperture is assumed. When the aperture size is smaller than the size of a pixel in the detector, light from an area where a pixel is enlarged by a factor of L can be collected. However, when the aperture size is comparable to the pixel size, it is not straightforward.

The signal S collected by the detector is an integral over the volume v from which radiation P enters the detector.

$$S = \int_v P(v)\frac{\Delta\Omega(v)}{4\pi}\mathrm{d}v, \tag{1}$$

where the $\Delta\Omega(v)$ is a solid angle of the pinhole looking from the plasma. When the $P(v)$ does not change so much perpendicular to the sight line, the volume integral can be written as a line integral,

$$S \sim \int_l P(s)\frac{\overline{\Delta\Omega(s)}}{4\pi}S(s)\mathrm{d}s, \tag{2}$$

$$= \int_l P(s)\frac{\overline{\Delta\Omega(s)}}{4\pi}4abL^2\mathrm{d}s, \tag{3}$$

where S(s) is the area of the detector projected on the plasma and ds is a line element on a sight line. Then we need to evaluate the averaged solid angle $\overline{\Delta\Omega(s)}$ from the plasma. The light from the plasma expands like a pyramid shape after it goes through the rectangular pinhole. Three cases when the light is collected are considered. (i) all light is collected, (ii) pyramid is on a side and (iii) pyramid is at a corner of the detector (Fig. 2 (a)). Corresponding area in the plasma side is shown in Fig. 2 (b). After calculating the solid angle from the plasma element, it is normalized by the projected area of the detector onto plasma ($4L^2ab$). Averaged solid angle from the plasma elements can be evaluated as $\overline{\Delta\Omega} = \frac{4ab}{(L+1)^2}(\frac{1}{3} + (1+\frac{1}{L})^2\frac{dc}{ab})$ [15].

From the compensation of $(L+1)^2$ with L^2 term, when $L >> 1$, the radiated power can be written as

$$S \sim \int_l P(s)\left[\frac{1}{3} + \left(1+\frac{1}{L}\right)^2\frac{dc}{ab}\right]\frac{16a^2b^2}{4\pi}\mathrm{d}s. \tag{4}$$

It is noted that the term $[\frac{1}{3} + (1+\frac{1}{L})^2\frac{dc}{ab}]$ is almost constant in the plasma in normal condition. We can get $S \sim C\int_l P(s)\mathrm{d}s$, where $C = [\frac{1}{3} + (1+\frac{1}{L})^2\frac{dc}{ab}]\frac{16a^2b^2}{4\pi}$ (5). This means that the signal is in proportional to the line integral of the local emission $P(s)$ along the sight lines. The tangentially viewed image can be thereby simulated numerically.

In order to simulate the image of toroidal plasmas viewed tangentially, we make an assumption that the SX radiation along the magnetic field line is constant. Then all elements along a line of sight can be mapped to elements in a reference poloidal plane (P2 in Fig. 3 (A)) by tracing the magnetic field lines. A column vector $\boldsymbol{S}$ ($S_i = 1, 2, \ldots, M$) representing measured signals can be thereby expressed as a linear combination of the radiation profile $\boldsymbol{P}$ ($P_i = 1, 2, \ldots, K$), geometrical weighing factor L and the residual error vector $\boldsymbol{e}$,

$$\boldsymbol{S} = L\boldsymbol{P} + \boldsymbol{e}. \tag{6}$$

By this relation we can simulate the tangentially viewed image $\boldsymbol{S}$ from local emission profile $\boldsymbol{P}$. Examples of the mapping of the line elements on a reference poloidal plane are shown in Fig. 3 (B)-(D).

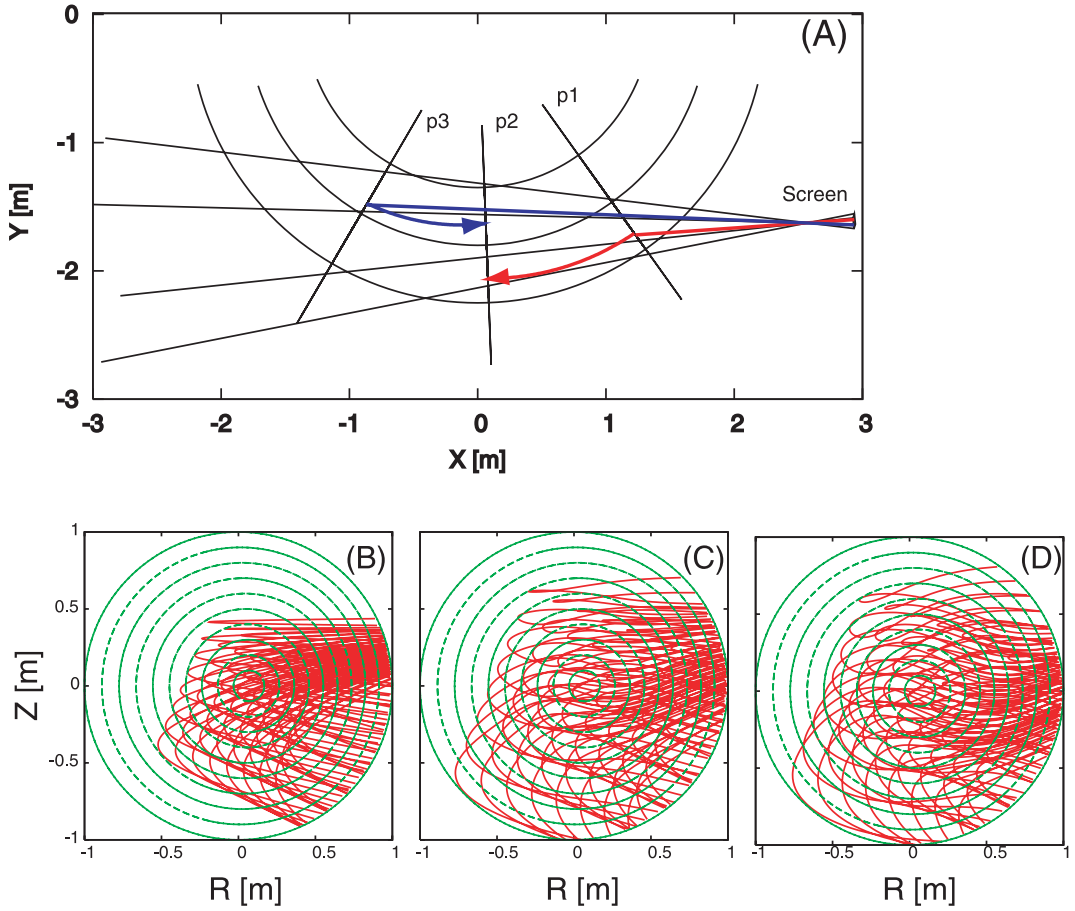

Fig. 3 Geometry of the tangentially viewing camera system on a toroidal system at the equatorial plane is shown in (A). Red and blue lines are drawn to show how the elements on sight lines at plane P1 or P3 are mapped to the elements on P2 following the magnetic field line. Mapping of the sight lines assuming no rotational transform (B), q_a = 9(C) and q_a = 3(D) are also shown. Here, q_a is the safety factor at the edge of the plasma.

From this drawing, the following facts can be seen. (I) The sight lines are deformed much when the rotational transform is large. (II) The projected images strongly depend on the equilibrium magnetic field; the error in the estimation of the equilibrium magnetic field is crucial.

When we need to reconstruct the image at the poloidal section, this condition becomes a severe constraint. When the estimation of the equilibrium field is good, we can do the reconstruction successfully [14] by solving equation (6) with Phillips-Tikhonov (PT) type regularization, it is not always possible. The error in the equilibrium magnetic field estimation at certain position might be large where the magnetic field shear is large. In this sense, the core of a Heliotron device (low magnetic shear and low rotational transform) and the edge of a tokamak plasma (low rotational transform and the error in the estimation is small) is favorable for this kind of tangential measurement.

Simulated image assuming the constant radiation along the magnetic field line is shown in Fig. 4 for the Large Helical Device (LHD) case. Measured image of the MHD instabilities observed in the experiments are shown together. In the core of the plasma, the similarity of the measured pattern and the image at the poloidal cross section is fairy good as we have estimated. When the structure is located in the edge region, the discrepancy of the measured signal and assumed pattern is large. In this case, detailed reconstruction of the image is required in order to interpret the measurements; the simplicity of the tangential imaging measurement is not fully brought out. It is also noted that the deformations of the equilibrium magnetic flux surface by the helical coil winding is also important for this disturbance of the line-integrated image in LHD. Interpretations of data are much difficult in these experimental conditions.

3. Tangentially Viewing VUV Telescope System

In this section, we describe a new type of the device, VUV telescope using the multi-layer mirror. The soft x-ray system we used so far had the advantage, that the photons it detects are in the same energy range as those emitted by the plasma. The drawback is, that no lenses are available in this energy range and we have to use a pinhole. Then the time and the space resolution are coupled. To improve the time resolution is then only possible if we increase the diameter

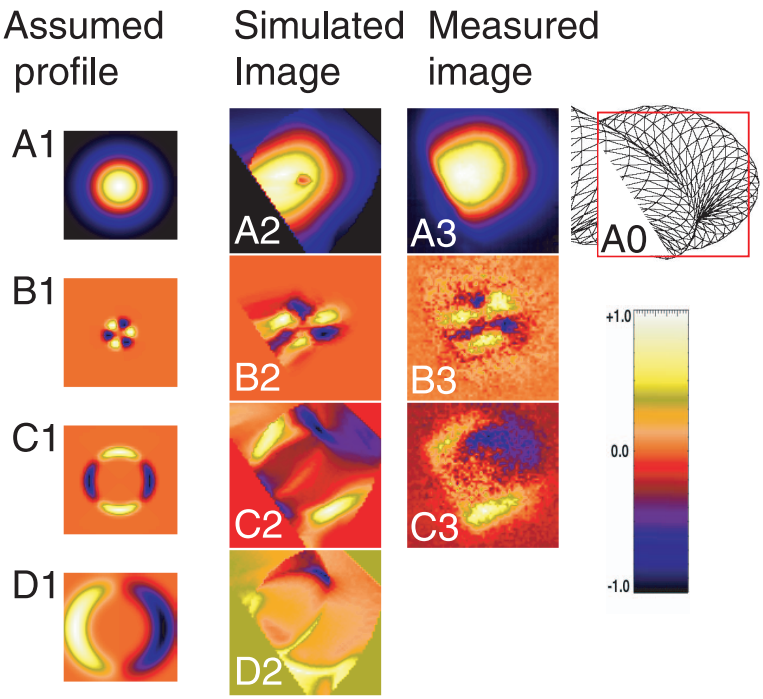

Fig. 4 Comparison of the images at a poloidal cross section (A1-D1) and simulated line-integrated image (A2-D2) assuming (A1-D1). Measured data in the experiments in LHD are also shown in (A3-C3). Left-bottom section is missing from the port arrangements as is shown in A0. Profiles of $\exp(-(\rho/0.5)^2)$, $\exp(-((\rho-0.2)/0.1)^2)\times\exp(-i3\theta)$, $\exp(-((\rho-0.55)/0.1)^2)\times\exp(-i2\theta)$ and $\exp(-((\rho-0.9)/0.1)^2)\times\exp(-i\theta)$ are assumed in Figure A, B, C and D respectively.

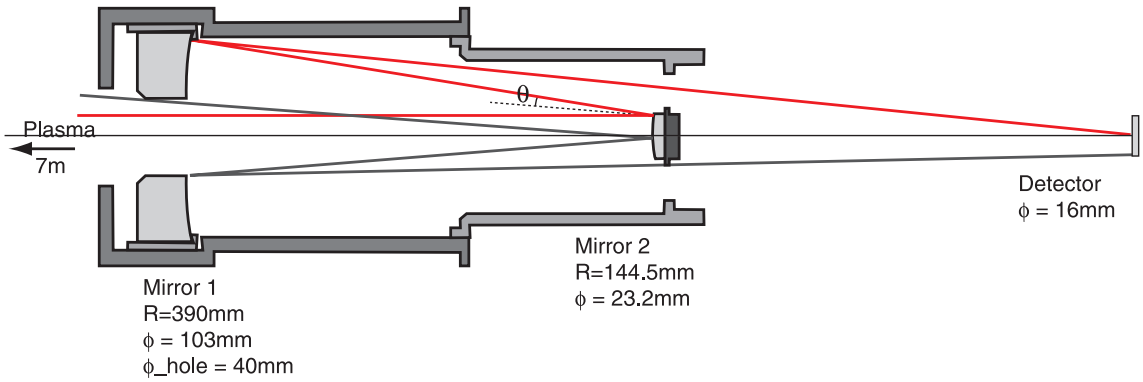

Fig. 5 Schematic view of the VUV telescope. Focal length = 7 m and the magnification of the system is 1/60.

of the pinhole and at the same time all sizes of the camera, i.e. also the size of the detector as we have discussed in the previous section. The size of the detector is, however, limited because of their availability; moreover, the camera becomes larger and needs more space on the experiment.

If we go to longer wavelength, the first optical components we can use are mirrors made of Mo-Be layers, which can reflect photon of 13.5 nm. The carbon VI line (13.5 nm) falls into this energy range. The reflectivity of the material is up to 65 % and the mirrors available are close to the theoretical limit. The CVI-line (n = 4-2) has been observed by the VUV spectrometer on LHD. Therefore we may expect to observe with the camera patterns in the boundary of fusion devices.

If we want to look further into the plasma, we have to provide for radiation in the energy range in which the camera works. This could be achieved e.g. by doping the neutral beams with carbon and use the charge exchange emission ($H^0 + C^{+6} \rightarrow H^+ + \left(C^{+5}\right)^*$). The emission cross section of the CVI is even larger for higher energy transitions [16]. We expect to study the core fluctuations by the impurity radiation when the neutral beam is injected [17].

Here, VUV telescope system we are developing is briefly described. We took the inverse-Schwarzschild type mirror optical system with a magnification of 1/60. A schematic drawing of the system is shown in Fig. 5. Ray-

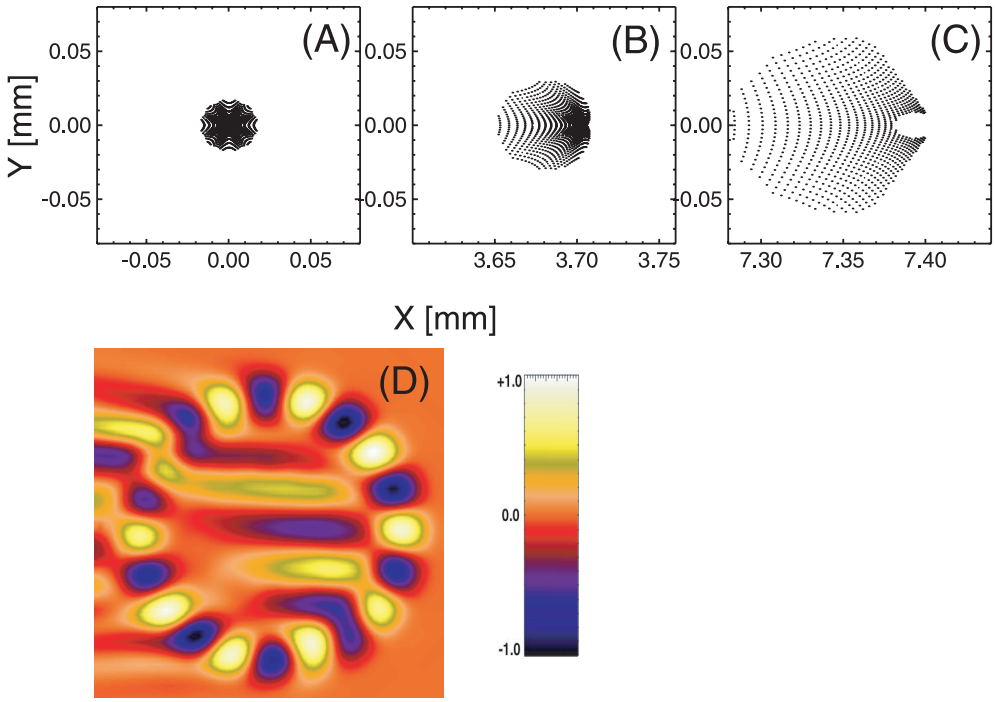

Fig. 6 Spot diagram of the mirror system at three positions (center (A), 2 cm and 4 cm from the center at focal point of the detector) are shown. Simulated line-integrated image of the fluctuations with a poloidal mode number m = 10 localized on $\rho = 0.5$ is also shown in (D).

tracing of the sight lines is done with this mirror system. The incident angle is calculated for the case where it is located at 7 m away from the plasma. It is less than 10 degree in this design and satisfies the restrictions posed by the mulit-layer mirror system. In Figure 6 (A)-(C), the intersection of the sightlines at the detector plane is shown as a spot diagram. Each ray starts from the point at the focus in the plasma. From the dispersion of the spot, the spatial resolution of the system is estimated. It is as small as $0.05\,\text{mm} \times 60 = 3\,\text{mm}$ in the middle of the viewing field. In the real experiment, the signal is a line integrated one. Estimate of the effective spatial resolution is therefore required. However, it strongly depends on the spatial structure of the fluctuations; systematic estimate is not easy. Here, a simulated image for a specific fluctuations (poloidal mode number $m = 10$ localized on $\rho = 0.5$) is shown in Fig. 6 (D). Up to poloidal mode numbers $m = 10$ can easily be resolved in case of a circular tokamak.

The effective brightness of the mirror system is also estimated. In the pinhole camera, the effective throughput of the system is evaluated by the factor C in the equation (5). It is shown in the Fig. 7 (A) as a function of the distance from the detector. If we replace the effective solid angle with the solid angle of the mirror viewed from the plasma, the effective throughput of the VUV camera system can also be shown. The size of the pinhole assumed here is 0.1 mm in order to get the similar spatial resolution obtained by the telescope system. It is 10^4 larger in the telescope system; we can expect a measurement with higher framing rate because we can collect more photons in the VUV telescope. The spot size at the center of the sight line is also shown in Fig. 7 (B). For small-scale fluctuations, comparable to the spot size, the image from far from the focal point is blurred by the finite depth of the focus. This is another advantage of the telescope system when we need to measure small-scale fluctuations. Together with good spatial resolution, we can expect to study the turbulence with scale lengths from several cm to several mm.

4. Summary

Merits of the tangential imaging for the visualization of the toroidally confined plasmas are discussed. The core of the Heliotron device (low magnetic shear and low rotational transform) and the edge of the tokamak plasma (low rotational transform) is favorable for measurements. A VUV telescope system in which the image formation is done by a mirror optics rather than by a pinhole is also proposed.

Acknowledgements

One of the author (S.O.) thanks the TEXTOR team and the LHD experimental group for the kind supports in the experiments. He appreciates Mr. K. Nagai of NTT Advanced Technology Corporation for the design of the mirror system. He also appreciate Prof. Y. Nagayama for his support in developing the VUV telescope system. This study is supported by NIFS budget code NIFS06ULHH509 and is also partially supported by the Ministry of Education, Science, Sports and Culture, Grant-in-Aid for Scien-

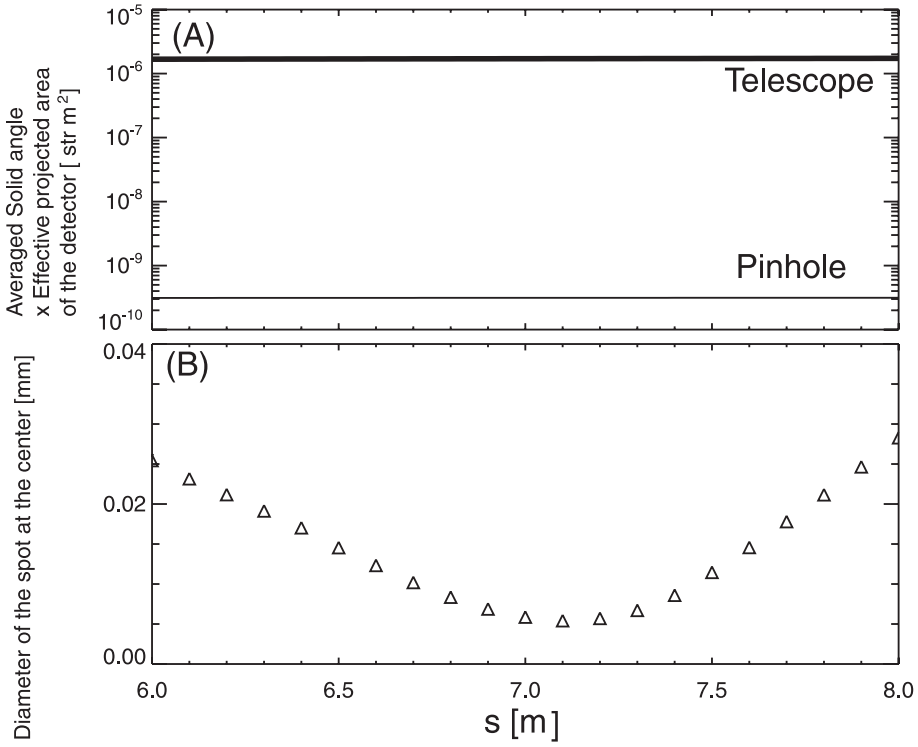

Fig. 7 The factor C as a function of the distant from the detector is shown in (A). The spot size as a function of the distant from the detector is also shown in (B).

tific Research (B), 17360446, 2005-. and the IAEA TEXTOR agreement (NIFS05KETE001).

[1] H.K. Park *et al.*, Phys. Rev. Lett. **96**, 195003 (2006).
[2] R.S. Granetz and P. Smeulders, Nucl. Fusion **28**, 457(1988).
[3] Y. Nagayama, S. Tsuji and K. Kawahata, Phys. Rev. Lett. **61**, 1839 (1988).
[4] M Antony *et al.*, Plasma Phys. Control. Fusion **38**, 1849 (1996).
[5] K. Ertl *et al.*, Nucl. Fusion **36**, 1477 (1996).
[6] A. Weller *et al.*, Rev. Sci. Instrum. **70**, 484 (1999).
[7] S. Ohdachi *et al.* , Rev. Sci. Instrum. **74**, 2136 (2003).
[8] S. von Goeler *et al.*, Rev. Sci. Instrum. **61**, 3055 (1990).
[9] S. Takamura, Nucl. Fusion **23**, 1485 (1983).
[10] R.J. Fonck, Nucl. Fusion **59**, 1831 (1988).
[11] S. von Goeler *et al.*, Rev, Sci, Instrum. **65**, 1621 (1994).
[12] D. Pacella *et al.*, Rev. Sci. Instrum. **72**, 1372 (2001).
[13] B.C. Stratton *et al.*, Rev. Sci. Instrum. **75**, 3959 (2004)
[14] S. Ohdachi, K. Toi, G. Fuchs, TEXTOR team and LHD experimental group, Plasma Science & Technology **8**, 45 (2006).
[15] S. Ohdachi, Doctor Theses (Nagoya University), 2003.
[16] R.C. Isler, Plasma Phys. Control. Fusion **36**, 171 (1994)
[17] D. Stutman *et al.*, Rev. Sci. Instrum. **77**, 10F330 (2006).